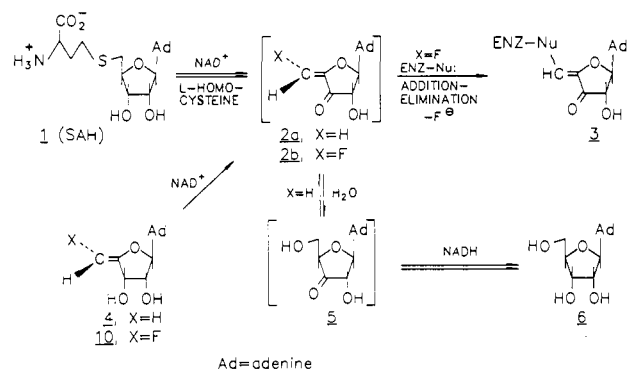
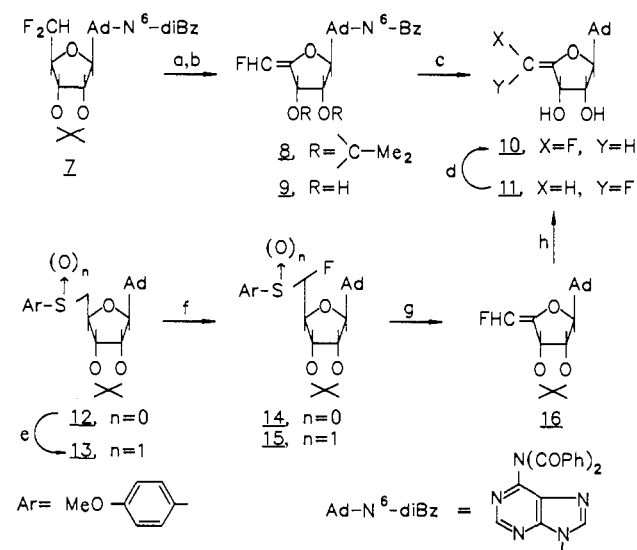


Scheme I. Mechanism of Action of SAH Hydrolase and the Incorporation of **4** and **10** into the Enzymatic Pathway**Scheme II^a**

^a Reagents: (a) KO-*t*-Bu, DMSO (59%); (b) 80% TFA, flash chromatography (*E*, 20%) (*Z*, 42%); (c) NH₃, EtOH (**10**, 61%) (**11**, 68%); (d) *hν*, sunlamp, acetone, MeOH (60%), (e) MCPBA (86%); (f) DAST; MCPBA (54%); (g) 140 °C, diglyme (77%); (h) 75% TFA, Dekker column (**10**, 48%) (**11**, 19%).

Table I. Kinetic Constants for SAH-Hydrolase Inhibitors

compound	K_1 (μM)	k_{inact} (min^{-1})	k_{inact}/K_1 ($\text{M}^{-1} \text{min}^{-1}$)
10	0.55	0.277	504 000
11	1.04	0.23	221 000

and the availability of crystalline enzyme,¹⁸ it may be possible to define the active site of the enzyme with these inhibitors.

Acknowledgment. We thank Dr. Jeffrey S. Wiseman and Professor Jeffrey Schwartz (Princeton University) for helpful discussions and advice. In addition, we thank Dr. Edward W. Huber and Robert J. Barbuch for spectral data and NOE experiments and Dr. Eugene R. Wagner for the purification of tritiated **10**.

Supplementary Material Available: Figure 1, which shows time- and concentration-dependent inhibition of SAH hydrolase by **10**, and experimental procedures and spectral data (NMR, IR, MS) for compounds **7**–**16** (12 pages). Ordering information is given on any current masthead page.

(18) Richards, H. H.; Chiang, P. K.; Cantoni, G. L. *J. Biol. Chem.* **1978**, *253*, 4476.

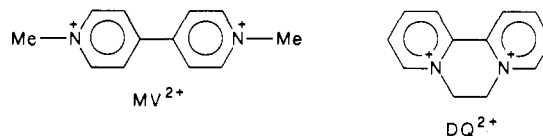
Shape-Selective Access to Zeolite Supercages. Arene Charge-Transfer Complexes with Viologens as Visible Probes

K. B. Yoon and J. K. Kochi*

Department of Chemistry, University of Houston
University Park, Houston, Texas 77204

Received October 17, 1988

Restricted yet ready access to the supercage represents an important facet of shape selectivity in zeolite catalysis.¹ However there is extant no general method to readily assess the structural constraints for the passage of hydrocarbon substrates in the liquid-phase through the zeolite framework. Our recent studies of intermolecular interactions² suggested that the stepwise assemblage of charge-transfer (CT) complexes directly within the zeolite cavity offers a viable approach to this problem. As a test case, we now report the shape-selective formation of various aromatic CT complexes in zeolites with the bipyridinium acceptors methylviologen MV²⁺ and diquat DQ²⁺ shown below.³



The cations MV²⁺ and DQ²⁺ are readily incorporated into zeolite-Y by ion exchange of Na⁺ at an 80% level of supercage occupancy.⁴ Mere exposure of these acceptor-doped colorless powders (400 mesh) to dilute solutions of anthracene, dimethylnaphthalene, and durene in dichloromethane leads immediately to distinctively colored purple, orange, and yellow zeolites, respectively, while the supernatant solutions remain colorless.⁵ The diffuse reflectance spectra of the colored zeolites show the presence of new bands that bear striking resemblance to the charge-transfer spectra of the corresponding arenes with MV²⁺ and DQ²⁺ in solution (Table I). Importantly, the absorption maxima (λ_{CT}) vary uniformly with the ionization potentials of different arene donors,⁸ and the linear correlation in Figure 1 confirms their charge-transfer character according to Mulliken.⁹ Furthermore, the subtle difference between the MV²⁺ and DQ²⁺ acceptors is clearly reflected in the displacement of the solid-state CT bands by an amount $\Delta h\nu_{\text{CT}}$ corresponding to the difference in their reduction potentials of $\Delta E_{\text{red}}^0 = 70 \text{ mV}$.¹⁰

The successful isolation of the bright orange, single crystal of the MV²⁺ complex with dimethoxynaphthalene allows X-ray crystallography (Figure 2)¹¹ to establish the relevant face-to-face

(1) (a) Breck, D. W. *Zeolite Molecular Sieves*; Wiley: New York, 1974. (b) Csicsery, S. M. *Zeolite Chemistry and Catalysis*; Rabo, J. A., Ed.; ACS Monograph 171, Washington, DC, 1976; p 680ff. (c) Weisz, P. B.; Frillette, V. J. *J. Phys. Chem.* **1960**, *64*, 382. (d) Herron, N. *Inorg. Chem.* **1986**, *25*, 4714. (e) Howe, R. F.; Lunsford, J. H. *J. Am. Chem. Soc.* **1975**, *97*, 5156. (f) Schoonheydt, R. A.; Pelgrims, J. J. *J. Chem. Soc., Dalton Trans.* **1981**, 914. (g) Winscom, C. J.; Lubitz, W.; Diegruber, H.; Moseler, R. *Stud. Surf. Sci. Catal.* **1982**, 12, 4.

(2) (a) Bockman, T. M.; Kochi, J. K. *J. Am. Chem. Soc.* **1988**, *110*, 1294. (b) Blackstock, S. C.; Kochi, J. K. *J. Am. Chem. Soc.* **1987**, *109*, 2484.

(3) (a) White, B. G. *Trans. Faraday Soc.* **1969**, *65*, 2000. (b) Poulos, A. T.; Kelley, C. K.; Simone, R. *J. Phys. Chem.* **1981**, *85*, 823. (c) Jones, I. G.; Malba, V. *Chem. Phys. Lett.* **1985**, *119*, 105.

(4) Typically, sodium zeolite-Y (Linde LZ-Y-52) was slurried with ~3 mM solutions of either MVCl₂ or DQBr₂ in water until 20% of Na⁺ was exchanged, and the colorless powder was then dried at 100 °C in vacuo (10⁻⁵ Torr) for 5 h.

(5) Such rapid uptake of arene is characteristic of doped zeolite supports to spread onto the active sites, reminiscent of those in solid solutions.^{6,7}

(6) Rabo, J. A.; Kasai, P. H. *Prog. Solid State Chem.* **1975**, *9*, 1.

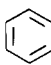

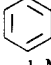
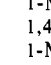
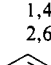
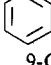
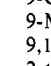
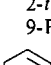


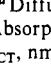
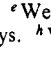

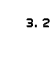

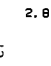

(7) Yoon, K. B.; Kochi, J. K. *J. Am. Chem. Soc.* **1988**, *110*, 6586.

(8) (a) Howell, J. O.; Goncalves, J. M.; Amatore, C.; Klasinc, L.; Wightman, R. M.; Kochi, J. K. *J. Am. Chem. Soc.* **1984**, *106*, 3968. (b) Schmidt, W. *J. Chem. Phys.* **1977**, *66*, 828.

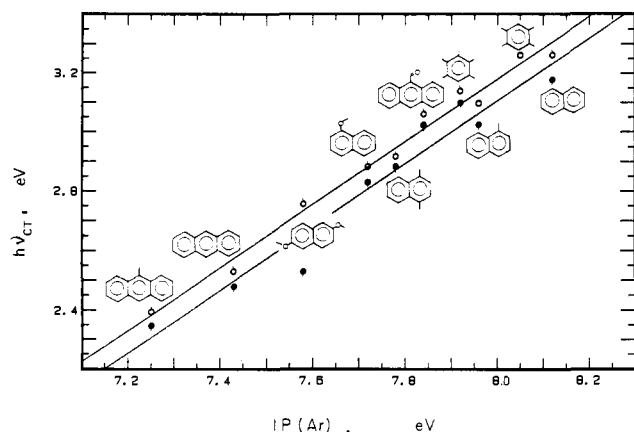
(9) (a) Mulliken, R. S. *J. Am. Chem. Soc.* **1950**, *72*, 601. (b) Mulliken, R. S.; Person, W. B. *Molecular Complexes*; Wiley: New York, 1969.

(10) (a) Bird, C. L.; Kuhn, A. T. *Chem. Soc. Rev.* **1981**, *10*, 49. (b) See: Foster (Foster, R. F. *Organic Charge-Transfer Complexes*; Academic: New York 1969) for the linear correlation of $h\nu_{\text{CT}}$ with E_{red}^0 .

Table I. Shape-Selective Formation of Arene CT Complexes with Bipyridinium Acceptors in Zeolite-Y

arene	IP (eV)	zeolite-Y ^a		solution ^b MV ²⁺
		MV ²⁺	DQ ²⁺	
 1,2,4,5-Me ₄	8.05	380	390	~360 ^c
 Me ₅	7.92	395	400	357
 Me ₆	7.85	none	none	385
	8.12	380	390	~360 ^c
 1-Me	7.96	400	410	~380 ^c
 1,4-Me ₂	7.78	425	430	410
 1-MeO	7.72	430	438	410
 1,4-(MeO) ₂	7.5	none ^d	none ^e	480 ^f
 2,6-(MeO) ₂	7.58	450	490	~430 ^c
	7.43	490	500	472
 9-CHO	7.84	405	410	~390 ^c
 9-Me	7.25	518	528	504
 9,10-Me ₂	7.11	none	none ^g	526
 2- <i>t</i> -Bu		none	505	484
 9-Ph	7.18	none	none	~500 ^c
	6.97	none	600	~590 ^h
	6.61	none	none	~600 ^h

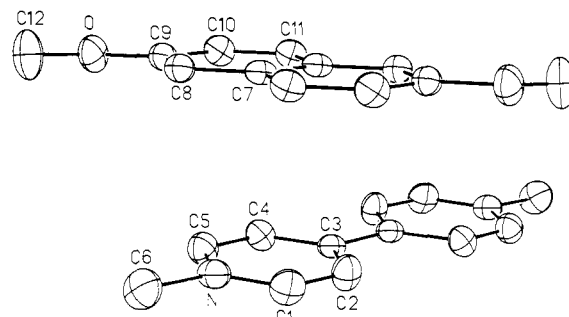
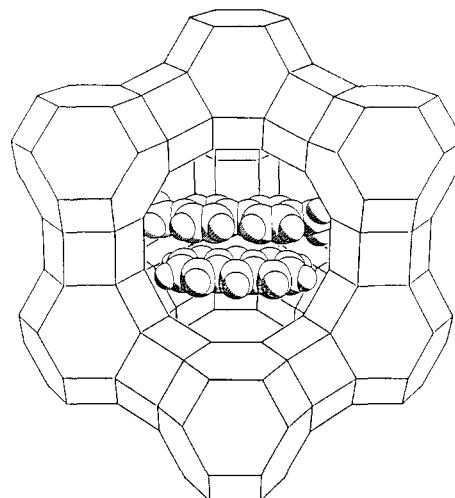
^a Diffuse reflectance spectrum (λ_{CT} , nm) as described in the text. ^b Absorption spectrum of arene CT complex with 75 mM MV(PF₆)₂ (λ_{CT} , nm) in acetonitrile. ^c Estimated (shoulder). ^d Weak CT after 15 h. ^e Weak CT only after 5 h. ^f Multiple band. ^g Weak CT after 3 days. ^h Very weak CT, alumina matrix.

**Figure 1.** Mulliken correlation of the diffuse reflectance spectra ($h\nu_{CT}$) of aromatic CT complexes in zeolite-Y doped with MV²⁺ (○) and DQ²⁺ (●).

interaction of the bipyridinium and arene planes leading to the charge-transfer absorption at $\lambda_{CT} = 450$ nm. Since the reflectance spectrum of this crystalline 1:1 complex is the same as that of the orange-colored zeolite, we conclude that the cofacial donor-acceptor arrangement is also relevant to that formed in the zeolite. If so, the zeolite cavity must be large enough to accommodate both the bipyridinium acceptor and the arene donor simultaneously.

Such steric restrictions are indicated in these zeolite experiments by the shapes of arene donors that can be accommodated. For example, all the methylbenzenes including mesitylene, durene,

(11) Crystal data for [MV(PF₆)₂, 2,6-(MeO)₂C₁₀H₆]: $M = 664.46$, monoclinic, space group $P2_1/c$, $a = 7.941$ (1) Å, $b = 11.459$ (2) Å, $c = 15.814$ (3) Å, $\beta = 103.57$ (1)°, $V = 1399$ Å³, $Z = 2$, Nicolet R3m/V diffractometer, Mo K α ($\lambda = 0.71073$ Å), $\mu = 2.54$ cm⁻¹, 1662 reflections $I > 3\sigma(I)$ refined to $R = 0.053$ ($R_w = 0.036$).

**Figure 2.** ORTEP perspective showing the parallel planes of the 2,6-dimethoxynaphthalene donor and MV²⁺ acceptor at a mean separation of 3.4 Å. For clarity, hydrogens and PF₆⁻ are not included.**Figure 3.** Pictorial representation of the "fit" within the zeolite-Y supercage of anthracene and methylviologen dication drawn to scale as parallel donor-acceptor pairs according to the CT structure in Figure 2.

and pentamethylbenzene rapidly form brilliant yellow CT complexes with MV²⁺ doped zeolite-Y, the single and striking exception being hexamethylbenzene that remains colorless. Likewise, the naphthalene derivatives in Table I yield bright yellow-to-orange zeolites—but the 1,4-dimethoxy and 2,6-di-*tert*-butyl derivatives leave the colorless zeolite unaltered. Shape selectivity is also manifested with anthracene by the rapid formation of the purple CT complex as well as with the 9-methyl and 9-formyl derivatives, but no colored zeolite obtains with either 9-phenyl or 9,10-dimethylanthracene and MV²⁺. Size distinction between the electron acceptors is readily brought out by 2-*tert*-butylanthracene and tetracene which both yield brightly colored zeolites with DQ²⁺, whilst the MV²⁺ doped zeolite-Y remains singularly unchanged.¹² The higher acene homologue pentacene does not form a CT complex in zeolite-Y with either DQ²⁺ or MV²⁺. It is important to emphasize that all of these arenes rapidly form the highly colored CT complexes with both MV²⁺ and DQ²⁺ when they are unrestricted in solution (see column 5, Table I).¹³

From the size exclusion of hexamethylbenzene (but not pentamethylbenzene), 9-phenyl- and 9,10-dimethylanthracene (but not 9-methylanthracene), and 1,4-dimethoxynaphthalene (but not the 2,6 isomer), we judge that a van der Waals "width" of roughly 8 Å¹⁴ is sufficient to inhibit an arene from complex formation with MV²⁺ immobilized in zeolite-Y. We believe that this represents the maximum value for the kinetic diameter σ^{15} of arenes in zeolite catalysis, and it accords with the 7.4 Å aperture to the supercage

(12) Note that MV²⁺ is 1.6 Å longer than DQ²⁺.

(13) The same CT complexes are also directly formed in the solid state by simply grinding the arene and MV(PF₆)₂ or DQ(PF₆)₂ with an alumina support.

(14) The widths are calculated from normal C-C and C-H bond distances and angles plus 0.8 Å for the extra van der Waals radius of hydrogen.

(15) Breck, D. W. ref 1a, p 340ff.

in zeolite-Y.¹⁶ [Note pentamethylbenzene with $\sigma = 7.15 \text{ \AA}$ passes readily, whereas hexamethylbenzene with $\sigma = 7.95 \text{ \AA}$ does not—despite its enhanced donor strength.] Once the arene has penetrated this window, a cavity dimension of $\sim 13 \text{ \AA}$ is large enough to accommodate both MV^{2+} and anthracene (but not tetracene), as depicted in Figure 3. A similar shape selectivity is also observed with zeolite-X (of related dimensions to zeolite-Y)¹⁷ but not with the more constricted 4.2 \AA aperture in zeolite-A¹⁸ or with completely amorphous silica alumina.

Owing to the wide structural variations that are allowed by different organic cations, we anticipate that shape selectivity can also be finely tuned in the formation of CT complexes with other types of hydrocarbon donors. We hope that further tests in progress will provide the requisite information for the detailed mapping of substrate access to various zeolite structures,¹⁹ especially with regard to both their kinetic and thermodynamic properties in the liquid phase.

Acknowledgment. We thank T. M. Bockman for helpful discussions, J. D. Korp for crystallographic assistance, and the National Science Foundation and Robert A. Welch Foundation for financial support.

Supplementary Material Available: Tables of data collection and processing parameters, atomic coordinates and isotropic displacement parameters, bond lengths and angles, and anisotropic displacement parameters (4 pages). Ordering information is given on any current masthead page.

(16) Breck, D. W. U. S. Patent 3,130,007 1964, [*Chem. Abstr.* 58, 7636] and p 177, ref 1a.

(17) Broussard, L.; Shoemaker, D. P. *J. Am. Chem. Soc.* 1960, 82, 1041.

(18) (a) Reed, T. B.; Breck, D. W. *J. Am. Chem. Soc.* 1956, 78, 5972. (b) Breck, D. W.; Eversole, W. G.; Milton, R. M.; Reed, T. B.; Thomas, T. L. *J. Am. Chem. Soc.* 1956, 78, 5963.

(19) See: Derouanne, E. G. *Diffusional Limitations and Shape Selective Catalysis in Zeolites*; Academic: New York, 1982.

Stark Effect Spectra of Ru(diimine)₃²⁺ Complexes

Dennis H. Oh and Steven G. Boxer*

Department of Chemistry, Stanford University
Stanford, California 94305

Received August 29, 1988

The metal-to-ligand charge-transfer (MLCT) states of Ru(diimine)₃²⁺ and related complexes have been the subject of intense interest over the past 20 years in an effort to understand and potentially to exploit their photochemical properties.¹ Although the degree of charge separation between the metal and ligand is the distinguishing characteristic of these states, little quantitative experimental data exists.² We report here the magnitude of the difference between the electric dipole moments of the ground and excited states, $|\Delta\mu_A|$, associated with MLCT transitions in several Ru(diimine)₃²⁺ complexes using Stark effect spectroscopy.

The effect of an applied electric field on the absorption spectrum (the Stark effect spectrum) has rarely been applied to the spectroscopy of transition-metal complexes; we are only aware of two examples in single crystals³ and none in solid solution as discussed in this communication.⁴ For a non-oriented sample in a rigid

(1) Juris, A.; Barigelletti, F.; Campagna, S.; Balzani, V.; Belsler, P.; von Zelewsky, A. *Coord. Chem. Rev.* 1988, 84, 85-277.

(2) The solvent dependence of absorption (or emission) band positions provides one approach to this problem. For example, see: Kober, E.; Sullivan, B. P.; Meyer, T. J. *Inorg. Chem.* 1984, 23, 2098-2104.

(3) (a) Solomon, E. I.; Ballhausen, C. J.; Høg, J. H. *Chem. Phys. Lett.* 1975, 34, 222-224. (b) Høg, J. H.; Ballhausen, C. J.; Solomon, E. I. *Mol. Phys.* 1976, 32, 807-814. (c) Johnson, L. W. *J. Chem. Phys.* 1983, 79, 1096-1097. We thank Professor Solomon for bringing these references to our attention.

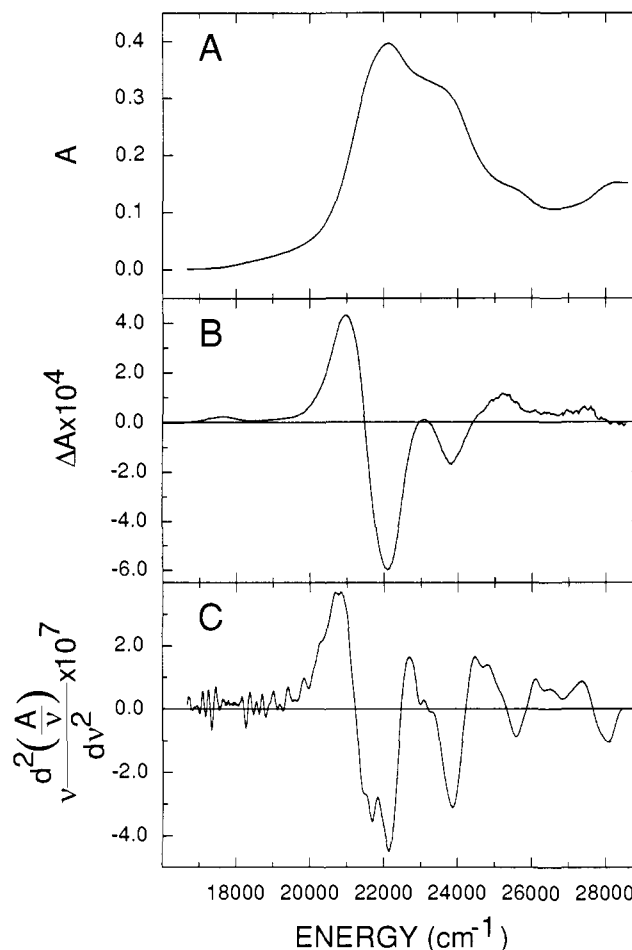


Figure 1. (A) Absorption spectrum of Ru(bpy)₃²⁺(PF₆)₂ in PVA at 77 K. (B) Stark effect spectrum of Ru(bpy)₃²⁺, $F_{\text{ext}} = 6.43 \times 10^5 \text{ V/cm}$; $\chi = 54.7^\circ$. (C) Second derivative of the absorption spectrum obtained by numerical differentiation. The Stark effect spectrum has the shape of the second derivative of the absorption spectrum in which each electronic absorption band is weighted by its appropriate value of $|\Delta\mu_A|^2$.⁵

matrix, the change in absorbance, ΔA , due to $\Delta\mu_A$ is proportional to the second derivative of the absorption line shape, the square of the electric field felt by the chromophore, and $|\Delta\mu_A|^2$.⁵

The absorption, second derivative of absorption, and Stark effect spectra of Ru(bpy)₃²⁺ (bpy = 2,2'-bipyridine) at 77 K are shown

(4) The molecule of interest is dissolved in a thin polymer film (typically 20–100 μm thick) that is coated with semitransparent electrodes across which an electric field is applied. For experimental details, see: Lockhart, D. J.; Boxer, S. G. *Biochemistry* 1987, 26, 664-668, 2958.

(5) More precisely

$$\Delta A(\nu) = \frac{C_x}{30h^2 F_{\text{int}}^2 \nu} \frac{d^2(A/\nu)}{d\nu^2}$$

where $C_x = \Delta\mu_A^2 [5 + (3 \cos^2 \chi - 1)(3 \cos^2 \zeta_A - 1)]$, χ is the angle between the applied electric field direction and the polarization vector of the probing beam, ζ_A is the angle between $\Delta\mu_A$ and the transition dipole moment being probed at energy $h\nu$, and F_{int} is the internal field related to the actual applied electric field, F_{ext} , by the local field correction: $F_{\text{int}} = fF_{\text{ext}}$. (Mathies, R. Ph.D. Thesis, Cornell University, 1974; Liptay, W. *Ber. Bunsenges.* 1976, 80, 207-217.) The value of f is generally greater than unity (typically about 1.2 for the polymers used here⁴); although its value is uncertain, it is likely to be roughly the same for different complexes in the same matrix and for different electronic states within a complex. For MLCT transitions, we assume $|\Delta\mu_A|$ dominates any effect due to a change in polarizability between the ground and excited states. The overall similarity between the Stark effect and second derivative of absorption line shapes confirms this. Figure 1 and the values of $|\Delta\mu_A|$ in Table I were obtained at $\chi = 54.7^\circ$ to minimize complications from variations in ζ_A due to overlapping bands, a problem that will be dealt with quantitatively elsewhere. The differential weighting of absorption bands by $|\Delta\mu_A|^2$ may help to reveal features that are obscured by overlapping bands. The signal-to-noise of the Stark data is far superior to that obtained by numerically differentiating the absorption spectrum.